

RESEARCH LETTER

10.1002/2017GL074881

Key Points:

- The A - β_{\parallel} relation for parallel propagating whistlers is obtained directly using quasilinear theory
- The saturation amplitude of broadband whistler waves can be predicted from the initial maximum linear growth rate
- The peak frequency and spectrum width of waves are well-defined functions of β_{\parallel} at saturation

Correspondence to:

X. Tao,
xtao@ustc.edu.cn

Citation:

Tao, X., L. Chen, X. Liu, Q. Lu, and S. Wang (2017), Quasilinear analysis of saturation properties of broadband whistler mode waves, *Geophys. Res. Lett.*, *44*, 8122–8129, doi:10.1002/2017GL074881.

Received 10 JUL 2017

Accepted 1 AUG 2017

Accepted article online 7 AUG 2017

Published online 19 AUG 2017

Quasilinear analysis of saturation properties of broadband whistler mode waves

X. Tao^{1,2} , L. Chen³ , X. Liu³ , Q. Lu^{1,2} , and S. Wang^{1,2}

¹CAS Key Laboratory of Geospace Environment, Department of Geophysics and Planetary Sciences, University of Science and Technology of China, Hefei, China, ²Collaborative Innovation Center of Astronautical Science and Technology, Harbin, China, ³Department of Physics, University of Texas at Dallas, Dallas, Texas, USA

Abstract Saturation properties of parallel propagating broadband whistler mode waves are investigated using quasilinear theory. By assuming that the electron distribution stays bi-Maxwellian, we combine the previously obtained energy equation of quasilinear theory with wave equation to self-consistently model the excitation of broadband whistler waves. The resulting evolution profile of wave intensity, spectrum, and electron temperature are consistent with those from particle-in-cell (PIC) simulations. We obtain the inverse relation between the saturation temperature anisotropy (A) and parallel plasma beta (β_{\parallel}) directly from quasilinear theory. Our A - β_{\parallel} relation agrees very well with previous results from observation and PIC simulation. We also demonstrate that it might be possible to predict the wave amplitude from the initial maximum linear growth rate alone and show that the peak frequency and spectrum width are well-defined functions of the final β_{\parallel} at saturation, but not of the initial β_{\parallel} .

1. Introduction

Whistler waves are important naturally occurring electromagnetic emissions in space plasmas [Helliwell, 1965]. These waves have been observed in the solar wind, magnetosheath, and planetary magnetospheres [e.g., Shaikh and Zank, 2010; Breneman et al., 2010; Stansby et al., 2016; Smith and Tsurutani, 1976; Tsurutani and Smith, 1974; Thorne et al., 1973]. Whistler waves play important roles in energetic electron dynamics in the inner magnetosphere. They can cause acceleration of a few hundred keV electrons and lead to the enhancement of MeV radiation belt electron fluxes during geomagnetically disturbed times [e.g., Horne and Thorne, 1998; Horne et al., 2005; Reeves et al., 2013] and precipitation of keV to a few tens of keV electrons to form diffuse aurora [Thorne et al., 2010], pulsating aurora [Nishimura et al., 2010], and pancake distributions [Tao et al., 2011].

Saturation properties of whistler mode waves are important to quantify related wave-particle interactions. Previous analysis of saturation properties of whistler mode waves has mainly used particle-in-cell (PIC) simulations [Gary and Wang, 1996; An et al., 2017]. The main advantage of PIC simulations is that all nonlinear wave-particle and wave-wave interactions are included. The main disadvantages of PIC simulations are that sometimes it is difficult to identify the main physical process and that simulations typically have high statistical noise. Saturation properties of broadband waves can also be analyzed using quasilinear theory [Kennel and Engelmann, 1966]. Yoon and Seough [2012] used quasilinear theory and obtained the anisotropy-beta relations for combined mirror and proton cyclotron instabilities for the case of $T_{\perp}/T_{\parallel} > 1$, where T is the temperature and subscripts “ \perp ” and “ \parallel ” denote perpendicular and parallel directions with respect to the background magnetic field. In a companion paper, Seough and Yoon [2012] reported the quasilinear analysis for parallel proton cyclotron instability for $T_{\perp}/T_{\parallel} > 1$ and parallel firehose instabilities for $T_{\perp}/T_{\parallel} < 1$. Kim et al. [2017] analyzed the electron temperature anisotropy regulation by whistler mode waves using quasilinear theory within the context of solar wind. In this study, we use quasilinear theory to analyze the saturation properties of broadband whistler mode waves.

Two kinds of saturation properties will be investigated. The first one is plasma properties at saturation, i.e., the inverse relation between temperature anisotropy ($A \equiv T_{\perp}/T_{\parallel} - 1$) and the parallel plasma beta ($\beta_{\parallel} \equiv 8\pi nT_{\parallel}/B^2$). Here n is the number density, and B is the magnetic field strength. Using linear theory analysis and assuming a bi-Maxwellian distribution for electrons, Gary and Wang [1996] pointed out that there

exists an upper bound on the electron temperature anisotropy due to the excitation of whistler mode waves, and the threshold temperature anisotropy satisfies the relationship

$$\frac{T_{\perp}}{T_{\parallel}} - 1 = S/\beta_{\parallel}^{\alpha}, \quad (1)$$

where S and α are two fitting constants. This constraint on A was then confirmed by 2-D PIC simulations [Gary and Wang, 1996]. However, in linear analysis, an assumption about the maximum linear growth rate (γ_m) is needed to obtain values for S and α . For example, assuming $\gamma_m = 0.01\Omega$, Gary and Wang [1996] found that $(S, \alpha) = (0.27, 0.57)$, and if $\gamma_m = 0.1\Omega$, the values of (S, α) change to $(0.58, 0.45)$. Here Ω is the unsigned electron cyclotron frequency. Using Cluster measurement, Gary *et al.* [2005] reported that the constraint on electron anisotropy upper bound in the magnetosheath is indeed given by equation (1) and for $0.1 \leq \beta_{\parallel} \leq 1.0$, $S \sim 0.2$, and $\alpha \sim 0.6$. Recently, Yue *et al.* [2016] used Van Allen Probes data and demonstrated that the electron temperature anisotropy constraint associated with excitation of whistler mode chorus waves is well described by equation (1). The upper bound of temperature anisotropy was demonstrated to be in good agreement with that from 2-D PIC simulations by An *et al.* [2017].

The other kind of properties to be investigated are the saturation properties of waves, including saturation amplitude, the peak frequency, and the spectrum width. These parameters are important to estimate the effects of waves on particle dynamics. The saturation amplitude, e.g., is a key parameter in determining the acceleration and loss time scale of energetic electrons in the inner magnetosphere [e.g., Kennel and Engelmann, 1966]. However, it is too time consuming with current computational power to use a PIC simulation code to obtain global distribution of whistler wave amplitudes in the magnetosphere. Bortnik *et al.* [2011] used local PIC simulations and demonstrated that the saturation amplitude of electromagnetic cyclotron ion waves (EMIC) can be described as a function of maximum k_{\parallel} , which is the imaginary part of the wave number k and is related to the linear growth rate γ by $k_{\parallel} = -\gamma/v_g$ with v_g the group velocity. This kind of mapping could be useful and important in global ring current simulations, which can give linear growth rate of waves but not saturation amplitude [Jordanova *et al.*, 2008]. Other properties (the peak frequency and the spectrum width) are also important properties in modeling of energetic electron dynamics [e.g., Glauert and Horne, 2005]. In this work, we use quasilinear theory to investigate the dependence of saturation wave amplitude, peak frequency, and the spectrum width on plasma parameters for whistler mode waves.

The remainder of the paper is organized as follows. In section 2, we briefly review quasilinear theory that will be used in this study and compare quasilinear results with PIC simulation results for a case study. In section 3, we perform quasilinear analysis for an ensemble of cases to obtain the inverse relationship between temperature anisotropy A and the saturation β_{\parallel} directly, and the dependence of the saturation amplitude, peak wave frequency, and spectrum width on plasma properties. We summarize our results in section 4.

2. Quasilinear Theory

2.1. Review of Quasilinear Theory

In this paragraph, we briefly review the quasilinear theory for parallel propagating waves and especially the energy equations of Ossakow *et al.* [1972] and describe how we use the equations to study the evolution and saturation properties of broadband whistler waves. The quasilinear equation describing the evolution of phase space density f is

$$\frac{\partial f}{\partial t} = \frac{q^2}{m^2} \sum_k |\mathbf{E}_k|^2 \left[\left(1 - \frac{kv_{\parallel}}{\omega_k^*}\right) \left(\frac{1}{v_{\perp}} \frac{\partial}{\partial v_{\perp}} v_{\perp}\right) + \frac{kv_{\perp}}{\omega_k^*} \frac{\partial}{\partial v_{\parallel}} \right] \quad (2)$$

$$\frac{i}{\omega_k - \Omega - kv_{\parallel}} \left[\left(1 - \frac{kv_{\parallel}}{\omega_k}\right) \frac{\partial}{\partial v_{\perp}} + \frac{kv_{\parallel}}{\omega_k} \frac{\partial}{\partial v_{\parallel}} \right] f, \quad (3)$$

where k is the wave number, q is the charge, m is the mass, \mathbf{E} is the electric field amplitude, v is the velocity, ω is the wave frequency, and ω_k^* is the complex conjugate of ω_k . Multiplying both sides by $mv_{\parallel}^2/2$ (or $mv_{\perp}^2/2$) and integrating overall velocities and assuming that the magnetic field energy dominates ($c^2k^2/\omega^2 \gg 1$), Ossakow *et al.* [1972] obtained

$$K_{\perp}(t) + \sum_k (|\mathbf{B}_k|^2/8\pi) \left[2 + \left(\omega_p^2/k^2c^2\right) \right] = C_{\perp}, \quad (4)$$

$$K_{\parallel}(t) - \sum_k (|\mathbf{B}_k|^2/8\pi) \left[1 + \left(\omega_p^2/k^2c^2\right) \right] = C_{\parallel}. \quad (5)$$

Here $K_{\perp,\parallel} = \langle mv_{\perp,\parallel}^2/2 \rangle$ are the average perpendicular and parallel kinetic energy of electrons, ω_p is the plasma frequency, c is the speed of light in vacuum, and \mathbf{B}_k is the magnetic field amplitude of the k_{th} mode. The two constants C_{\perp} and C_{\parallel} depend only on the initial conditions. Equations (4) and (5) essentially describe the transfer of perpendicular kinetic energy to the wavefield and the parallel kinetic energy, as whistler waves are driven unstable. As wave energy grows, K_{\perp} decreases and K_{\parallel} increases, or A decreases and β_{\parallel} increases. This is the quasilinear relaxation of the electron temperature anisotropy by interactions with whistler mode waves. For other details of the theory, we refer the readers to *Ossakow et al.* [1972].

In equations (4) and (5), the parallel and perpendicular average kinetic energy are related to the corresponding temperature by $T_{\perp} \equiv m\langle v_{\perp}^2 \rangle/2 = K_{\perp}$ and $T_{\parallel} \equiv m\langle v_{\parallel}^2 \rangle = 2K_{\parallel}$. Within the quasilinear framework, the wave growth is described by linear theory; therefore, the equation describing wave energy evolution of the k_{th} mode is simply

$$\frac{\partial |\mathbf{B}_k|^2}{\partial t} = 2\gamma_k |\mathbf{B}_k|^2, \quad (6)$$

where γ_k is the linear growth rate of the k_{th} mode. If we assume that the distribution stays bi-Maxwellian [Gary and Wang, 1996; Yoon and Seough, 2012; Seough and Yoon, 2012], then γ_k can be calculated directly from the parallel and perpendicular temperature. Taking the time derivative of equations (4) and (5), we have the needed differential equations to describe the time evolution of the electron temperature

$$\frac{dT_{\perp}}{dt} = - \sum_k 2\gamma_k \frac{|\mathbf{B}_k|^2}{8\pi} \left[2 + \left(\omega_p^2/k^2 c^2 \right) \right], \quad (7)$$

$$\frac{dT_{\parallel}}{dt} = \sum_k 4\gamma_k \frac{|\mathbf{B}_k|^2}{8\pi} \left[1 + \left(\omega_p^2/k^2 c^2 \right) \right]. \quad (8)$$

Similar equations have been derived by *Seough and Yoon* [2012] for EMIC waves.

Equations (6)–(8) are the main equations used in this study to analyze excitation and saturation of whistler mode waves. We choose 100 k 's, corresponding to those of whistler mode waves with frequency between 0.05Ω and 0.95Ω , and assume a small initial noise level (e.g., by setting $|\mathbf{B}_k|^2 = 10^{-5}$ for all k 's). Then by solving the closed set of equations (6)–(8), we self-consistently track the evolution of whistler waves and the parallel and perpendicular temperature of electrons based on quasilinear theory.

2.2. A Case Study

Figure 1 shows an example of the quasilinear analysis results, chosen from the ensemble runs in section 3. The initial $A = 1.67$, $\beta_{\parallel} = 0.278$, and $\omega_{pe}/\Omega = 8$. Figure 1 (top left) shows the evolution of K_{\perp} and K_{\parallel} normalized by $C_t \equiv C_{\perp} + C_{\parallel}$. Because of the small initial noise level of \mathbf{B}_k , $C_{\perp,\parallel} \approx K_{\perp,\parallel}(t = 0)$. Figure 1 (bottom left) shows the evolution of the normalized wave magnetic field intensity. In the initial linear growth phase, the wave energy quickly increases and saturates near $t \approx 80\Omega^{-1}$. At the same time, the perpendicular kinetic energy decreases and the parallel kinetic energy increases. This kind of evolution of particle energy and wave energy is consistent with previous PIC simulations [Gary and Wang, 1996]. After saturation ($t \approx 80\Omega^{-1}$), all three quantities change very slowly.

Figure 1 (top right) shows the evolution of the wave spectrum, and Figure 1 (bottom right) shows the linear growth rate as a function of ω and t . In the linear growth phase, the excited spectrum is between $\sim 0.25\Omega$ and about $\sim 0.6\Omega$, consistent with the range of the initial positive linear growth rate. After $t \approx 50\Omega^{-1}$, the wave intensity, $(\delta B/B)^2$, has increased to about 10^{-2} , and the range of the frequency spectrum and the positive range of linear growth rate quickly shift toward the lower frequency range. This is because the relaxation of the temperature anisotropy reduces the maximum frequency of positive linear growth rate, which is given by $\omega_m/\Omega = A/(1+A)$ [Kennel and Petschek, 1966; Ossakow et al., 1972]. Note that nonlinear wave-wave coupling is not included in quasilinear theory; therefore, the shift of the spectrum is purely due to the change of the equilibrium distribution function.

2.3. Comparison Between Quasilinear Analysis and PIC Simulation

Before we analyze the saturation properties of broadband whistler mode waves, we compare the evolution of wave energy between PIC simulation and quasilinear theory for a case. Here we use a one-dimensional electromagnetic PIC simulation code [Tao and Lu, 2014; Tao, 2014], where field quantities are assumed to vary along z direction and three components of the velocity are retained. Only parallel propagating whistler mode waves are allowed, consistent with the assumption used in our quasilinear analysis. The electron distribution

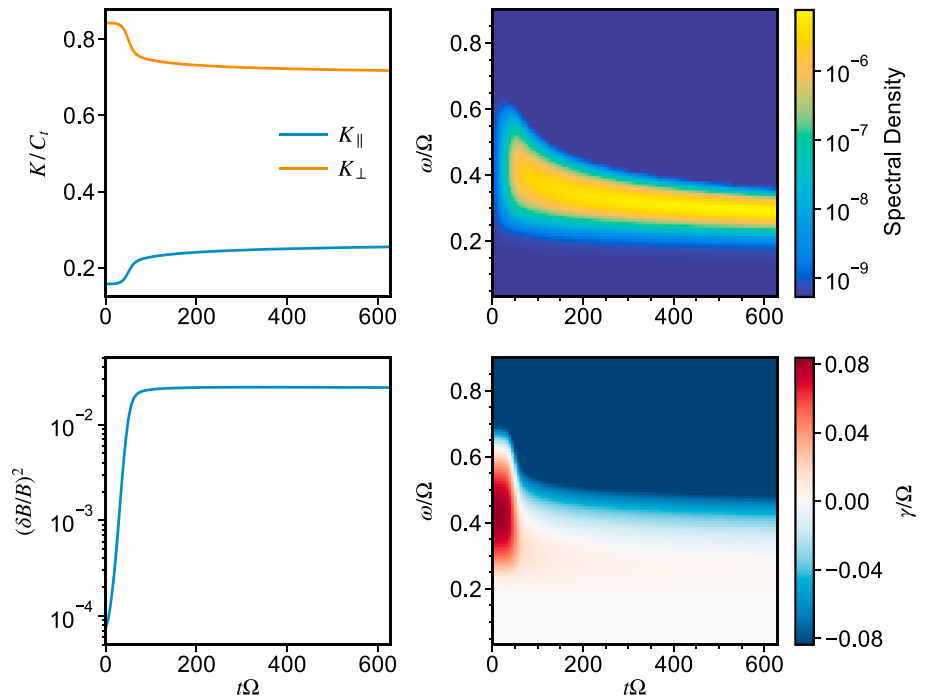


Figure 1. Results from quasilinear analysis: (top left) evolution of parallel and perpendicular average kinetic energy, (top right) evolution of the wave spectrum, (bottom left) time evolution of the normalized wave intensity, and (bottom right) time evolution of the linear growth rate.

used in the PIC simulation is a single bi-Maxwellian. For the case in this section, the simulation parameters are taken from *Ossakow et al. [1972]*. We use $T_{\perp}/T_{\parallel} = 4$, $\omega_{pe}/|\Omega_e| = 2$, and $w_{\parallel}/c = 0.07$, where w_{\parallel} is the parallel thermal velocity. For this PIC simulation, we use 1024 simulation cells and 2000 number of particles per cell. The cell size is $\Delta z = 0.05c/\Omega$, and the time step is $\Delta t = 0.02 \Omega^{-1}$.

Figure 2 shows the evolution of wave intensity from PIC simulation and the quasilinear analysis. The initial noise level of the wavefield in quasilinear analysis is chosen to roughly match that of the PIC simulation. We fit the linear growth phase of the wave intensity from PIC simulation and quasilinear analysis by $C_0 \exp^{C_1 t}$, where C_0 and C_1 are two constants. Clearly, $C_1 = 2\bar{\gamma}$, where $\bar{\gamma}$ is the average linear growth rate. From Figure 2, $\bar{\gamma}/\Omega \approx 0.025$ for PIC simulation and 0.035 for quasilinear analysis. The difference of the saturation intensity between quasilinear theory analysis and the PIC simulation is within a factor of 2. Considering the approximations made in the quasilinear analysis, we conclude that results from the quasilinear analysis roughly agree with those from PIC simulation, and that quasilinear theory can roughly capture the main physical process in the evolution of broadband whistler mode waves.

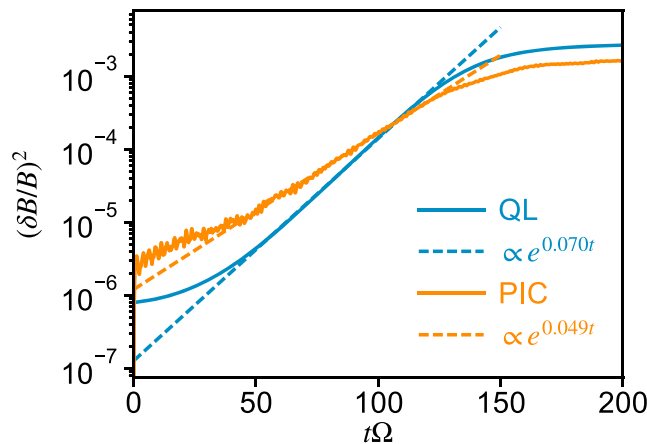


Figure 2. Comparison between quasilinear results (solid blue lines) and PIC simulation results (solid orange lines). Dashed lines denote the power law fitting to the linear growth phase.

3. Saturation Properties of Broadband Whistler Mode Waves

In this section, we apply the quasilinear analysis to an ensemble of cases to obtain statistically the saturation properties of broadband whistler mode waves. In all following analysis, we use 10 initial β_{\parallel} 's logarithmically evenly

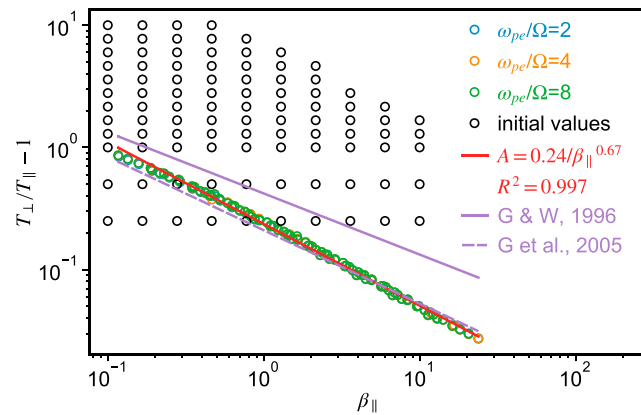


Figure 3. The A - β_{\parallel} relation at saturation from quasilinear analysis. The solid red line is the fitting using $A = S/\beta_{\parallel}^{\alpha}$. Black circles denote initial conditions, while color circles denote saturation conditions. The solid purple line denotes the A - β_{\parallel} relation from PIC simulation results from Gary and Wang [1996], the dashed purple line from Gary et al. [2005].

selected cases have very large initial linear growth rate, and we have removed all cases with $\gamma_{0m}/\Omega > 1$, where γ_{0m} is the maximum initial linear growth rate. For all cases, we solve equations (6)–(8) from $t\Omega = 0$ to 600 and verify that the wavefield has reached the saturation stage.

3.1. The A - β_{\parallel} Relationship

Previous studies based on linear theory [Gary and Wang, 1996], PIC simulation [An et al., 2017], or observation [Gary et al., 2005; Yue et al., 2016] have suggested that the saturation A - β_{\parallel} relation for whistler mode waves should satisfy equation (1). As discussed in section 1, linear theory cannot determine the value of S or α in equation (1), because the distribution is assumed to be the unperturbed initial distribution all the time. On the other hand, as having been demonstrated, quasilinear theory can directly give A and β_{\parallel} at saturation.

Figure 3 shows A and β_{\parallel} at $t = 0$ and after wave saturation for all cases calculated. It clearly shows that the final A - β_{\parallel} relation from quasilinear theory can be well fit by equation (1) with $S = 0.24$ and $\alpha = 0.67$, and fitting parameters S and α are independent of ω_{pe}/Ω . To quantify the goodness of regression, we use the R^2 parameter, which is defined by

$$R^2 = 1 - \frac{\sum_i (y_i - f_i)^2}{\sum_i (y_i - \langle y_i \rangle)^2}, \quad (9)$$

where y_i is the i th value of the dependent variable, f_i is the value of the fitting function for the i th independent variable x_i , and $\langle y_i \rangle$ is the mean value of y_i . For the current case, $y = A$, $x = \beta_{\parallel}$, and $f = 0.24/\beta_{\parallel}^{0.67}$. The parameter R^2 takes value between 0 and 1. An R^2 of 1 suggests that the regression line perfectly fits the data. For this case, $R^2 = 0.997$ suggests that $A = 0.24/\beta_{\parallel}^{0.67}$ can well describe the relationship between A and β_{\parallel} at saturation.

For comparison, we also plot the $A = S/\beta_{\parallel}^{\alpha}$ line with $S = 0.42$ and $\alpha = 0.50$ from Gary and Wang [1996], and $S = 0.21$ and $\alpha = 0.60$ from Gary et al. [2005]. As can be seen, the quasilinear results agree surprisingly well with those from Gary et al. [2005], based on Cluster observations in the magnetosheath. Compared with Gary and Wang [1996], our temperature anisotropy upper bound is smaller by about 0.05 for $\beta_{\parallel} \sim 0.1$ and about 0.2 for $\beta_{\parallel} \sim 20$. Note that the temperature anisotropy upper bound from 2-D PIC simulation results from An et al. [2017] are consistently lower than the one from Gary and Wang [1996] by about $0.1 \sim 0.2$ for $10^{-1} \leq \beta_{\parallel} \lesssim 4$; therefore, we conclude that the quasilinear theory results agree very well with PIC simulation results for this β_{\parallel} range. Our analysis suggests that the saturation A - β_{\parallel} relation can be well described by quasilinear theory for this β_{\parallel} range, even though we assumed that the distribution stays bi-Maxwellian.

3.2. The Dependence of the Saturation Wave Properties on Plasma Parameters

In this section, we investigate the dependence of the saturation wave amplitude, the peak frequency, and spectrum width at saturation on plasma parameters.

spaced between 10^{-1} and 10. This range of β_{\parallel} has been used by Gary and Wang [1996]. We do not use smaller β_{\parallel} , because previous studies [e.g., Gary et al., 2011] have demonstrated that, for $\beta_{\parallel} \lesssim 0.02$, the excited whistler mode waves are predominately oblique, therefore not consistent with our assumption that parallel propagating waves dominate the spectrum. We select 12 initial A 's. There are 10 logarithmically evenly spaced A 's between 10^0 and 10^1 . We add $A = 0.25$ and 0.5 so that some of the initial conditions (A, β_{\parallel}) fall below the final threshold A - β_{\parallel} line, as will be seen below. We also select three ratios of plasma frequency to cyclotron frequency ($\omega_{pe}/\Omega = 2, 4$, and 8) to test the dependence of saturation properties on ω_{pe}/Ω . Some of the

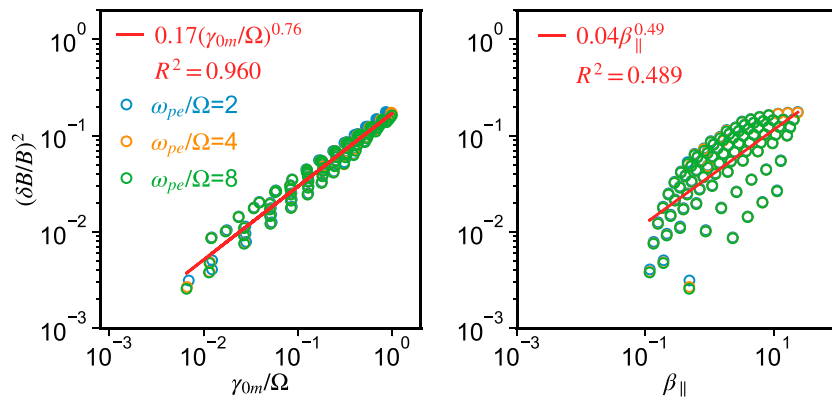


Figure 4. The normalized saturated wave magnetic field energy as a function of the initial (left) γ_{0m} and the (right) β_{\parallel} at saturation.

Figure 4 (left) shows the normalized saturation intensity as a function of maximum initial linear growth rate, γ_{0m} . We fit the saturation amplitude using a power law function, and the resulting fitting function is $0.17(\gamma_{0m}/\Omega)^{0.76}$. Note that there is larger spread at smaller γ_{0m} . However, for a given γ_{0m} , the difference between maximum and minimum saturation intensity is within a factor of 2.

An *et al.* [2017] used 2-D PIC simulation and investigated the relationship between the saturation wave intensity with β_{\parallel} at saturation. Here we present the quasilinear results for this relation. Figure 4 (right) shows the dependence of saturation wave intensity as a function of β_{\parallel} at saturation. We fit the saturation intensity as a function of β_{\parallel} using a power law function, following An *et al.* [2017]. The $(\delta B/B)^2$ scales with β_{\parallel} roughly as $\beta_{\parallel}^{0.5}$. The slope 0.5 is smaller than that obtained by An *et al.* [2017], which is about 1.5–2. However, note that the main range of the saturation β_{\parallel} is from about 0.1 to 100 in this work, while the range in An *et al.* [2017] is from 10^{-2} to ~ 3 . In the larger β_{\parallel} region ($\beta_{\parallel} > 0.1$) of An *et al.* [2017] results, the power law index is apparently

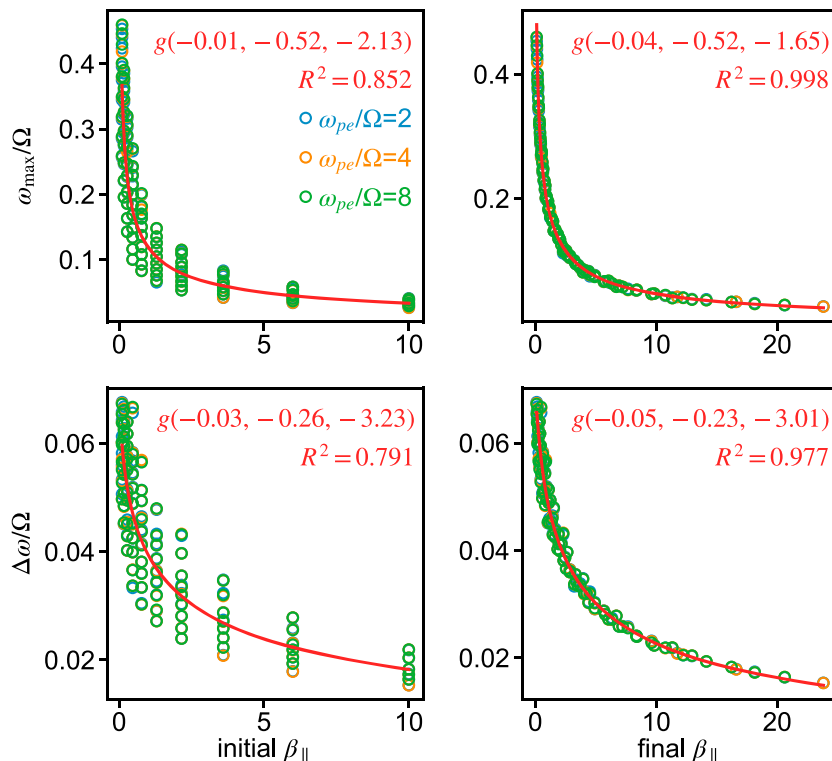


Figure 5. The (top row) peak wave frequency and the (bottom row) spectrum width as a function of the (left column) initial β_{\parallel} and the (right column) final β_{\parallel} . Red lines are fitting functions using the form given by equation (10).

much smaller than 2. If we only compare the saturation intensity for $0.1 \leq \beta \leq 3$, we see that the saturation intensity $(\delta B/B)^2$ is consistent with that from *An et al.* [2017]. For example, from *An et al.* [2017], $(\delta B/B)^2$ is on the order of 10^{-3} for $\beta_{\parallel} = 10^{-1}$ and on the order of 10^{-2} for $\beta_{\parallel} = 1$. These values are very close to quasilinear results shown in Figure 4. Comparing Figure 4 (left and right), we conclude that it might be possible to predict $(\delta B/B)^2$ based on γ_{0m} , but not β_{\parallel} at saturation, since $(\delta B/B)^2$ is not a well-defined single-value function of β_{\parallel} .

Figure 5 shows the normalized peak frequency ω_{\max}/Ω and the spectrum width $\Delta\omega/\Omega$ as a function of the initial β_{\parallel} and the final β_{\parallel} . Denoting the wave power spectral density as $P(\omega)$, the peak frequency is the frequency with maximum intensity, i.e., $P_{\max} = P(\omega_{\max})$. The spectrum width, $\Delta\omega$, is defined as the difference between two frequencies ω_1 and ω_2 which satisfy $P(\omega_1) = P(\omega_2) = P_{\max}/10$. From Figure 5, both ω_{\max} and $\Delta\omega$ are better correlated with β_{\parallel} at saturation than with initial β_{\parallel} . After some experimentation, we choose to fit data using the analytical function of the following form:

$$g(a, b, c) = \exp [a(\ln \beta_{\parallel})^2 + b \ln \beta_{\parallel} + c]. \quad (10)$$

The corresponding parameters are shown in Figure 5 for all four panels. The R^2 parameters are close to 1 for Figure 5 (right column), suggesting that the chosen function g can almost perfectly describe the relationship between ω_{\max} and $\Delta\omega$ as a function of the final β_{\parallel} . From Figure 5 (left column), the peak frequency and the frequency width cannot be well predicted from the initial β_{\parallel} . We have also experimented with initial γ_{0m} and the initial A , both parameters give even worse results than the initial β_{\parallel} .

4. Summary

In this work, we used quasilinear theory to analyze the saturation properties of parallel propagating broadband whistler mode waves in a plasma where electrons have a single bi-Maxwellian distribution. Specifically, we investigated the A - β_{\parallel} relationship and the dependence of saturation amplitudes, peak frequency, and frequency width on initial linear properties and the saturation β_{\parallel} . Using self-consistent quasilinear analysis, the obtained A - β_{\parallel} relation agrees very well with observations in the magnetosheath using Cluster measurement [*Gary et al.*, 2005]. Our A - β_{\parallel} relation also agrees with recent 2-D PIC simulations and the Van Allen Probes observation in the high β_{\parallel} ($\beta_{\parallel} > 0.1$) regime [*Yue et al.*, 2016]. Unlike linear theory [*Gary and Wang*, 1996], there is no need to choose an initial maximum linear growth, and the inverse relationship between A and β_{\parallel} is directly given in quasilinear theory. Compared with PIC simulation, the quasilinear theory analysis does not suffer from high statistical noise, and it helps to identify that the main physical process involved in the evolution and saturation of broadband whistler mode waves can be well described by quasilinear theory.

We investigated the relationship between saturation amplitude $(\delta B/B)^2$ and the maximum initial linear growth rate γ_{0m} and β_{\parallel} at saturation. We showed that it is possible to predict $(\delta B/B)^2$ from initial γ_{0m} . This conclusion might be useful when predicting whistler mode wave amplitude from global non-self-consistent wave modeling codes, such as the ring current and atmosphere interactions model (RAM) code [*Jordanova et al.*, 2010]. And therefore, our results might be useful in coupling microphysical processes with global macroscopic simulations. We also compared $(\delta B/B)^2$ as a function of β_{\parallel} at saturation from our quasilinear results with recent 2-D PIC simulations [*An et al.*, 2017], and we found that the two results agree well with each other for $\beta_{\parallel} > 0.1$.

We demonstrated that the peak frequency and the spectrum width are well-defined functions of β_{\parallel} at saturation, but not of the initial β_{\parallel} . We showed that both ω_{\max} and $\Delta\omega$ might be modeled as a function of β_{\parallel} at saturation using analytical form $g(a, b, c) = \exp[a(\ln \beta_{\parallel})^2 + b \ln \beta_{\parallel} + c]$, where a , b , and c are the three parameters. The R^2 parameters for both fittings are close to 1.

Finally, we would like to discuss the limitations of this work and the extensions that can be made. The main limitation of this work is that the electron distribution is assumed to stay as bi-Maxwellian throughout the wave excitation, so that the linear growth rate can be directly calculated using T_{\perp} and T_{\parallel} . As pointed out by *Yoon and Seough* [2012], this can be regarded as the lowest-order approximation. Our results, as discussed above, turn out to agree very well with observations and PIC simulations, despite of this assumption. There are at least two extensions to this work that can be made in the future. First, we considered only high- β_{\parallel} region so that parallel whistler mode waves dominate the spectrum, consistent with the assumption used in the quasilinear analysis. In the low β_{\parallel} region ($\beta_{\parallel} < 0.02$), oblique whistler waves should become much more important [*Gary et al.*, 2011]. Correspondingly, to extend our work to low β_{\parallel} region, one would have to incorporate excitation of oblique waves and use 2-D quasilinear analysis. Second, in the inner magnetosphere, electron distribution

typically has a cold component and a hot component. To make our results more applicable to the inner magnetosphere, a cold electron component needs to be added to the analysis. Note that adding a cold electron component is expected to lower the anisotropy constraint and saturation amplitude but not to change the scaling law obtained in this study [Gary and Wang, 1996].

Acknowledgments

This work was supported by NSFC grants 41631071, 41474142, 41674174, and 41421063. We thank Xin An for helpful discussions regarding his PIC simulation results and an anonymous reviewer for pointing out the work of Kim *et al.* [2017], which we were not aware of before. The model data will be preserved on a long-term storage system and will be made available upon request to the corresponding author.

References

- An, X., C. Yue, J. Bortnik, V. Decyk, W. Li, and R. M. Thorne (2017), On the parameter dependence of the whistler anisotropy instability, *J. Geophys. Res. Space Physics*, *122*, 2001–2009, doi:10.1002/2017JA023895.
- Bortnik, J., N. Omidi, L. Chen, R. M. Thorne, and R. B. Horne (2011), Saturation characteristics of electromagnetic ion cyclotron waves, *J. Geophys. Res.*, *116*, A09219, doi:10.1029/2011JA016638.
- Breneman, A., C. Cattell, S. Schreiner, K. Kersten, L. B. Wilson, P. Kellogg, K. Goetz, and L. K. Jian (2010), Observations of large-amplitude, narrowband whistlers at stream interaction regions, *J. Geophys. Res.*, *115*, A08104, doi:10.1029/2009JA014920.
- Gary, S. P., and J. Wang (1996), Whistler instability: Electron anisotropy upper bound, *J. Geophys. Res.*, *101*(A5), 10,749–10,754.
- Gary, S. P., B. Lavraud, M. F. Thomsen, B. Lefebvre, and S. J. Schwartz (2005), Electron anisotropy constraint in the magnetosheath: Cluster observations, *Geophys. Res. Lett.*, *32*, L13109, doi:10.1029/2005GL023234.
- Gary, S. P., K. Liu, and D. Winske (2011), Whistler anisotropy instability at low electron β : Particle-in-cell simulations, *Phys. Plasmas*, *18*(8), 082902, doi:10.1063/1.3610378.
- Glauert, S. A., and R. B. Horne (2005), Calculation of pitch angle and energy diffusion coefficients with the PADIE code, *J. Geophys. Res.*, *110*, A04206, doi:10.1029/2004JA010851.
- Helliwell, R. A. (1965), *Whistlers and Related Ionospheric Phenomena*, Stanford Univ. Press, Stanford, Calif.
- Horne, R. B., and R. M. Thorne (1998), Potential waves for relativistic electron scattering and stochastic acceleration during magnetic storms, *Geophys. Res. Lett.*, *25*(15), 3011–3014.
- Horne, R. B., et al. (2005), Wave acceleration of electrons in the Van Allen radiation belts, *Nature*, *437*, 227–230, doi:10.1038/nature03939.
- Jordanova, V. K., J. Albert, and Y. Miyoshi (2008), Relativistic electron precipitation by EMIC waves from self-consistent global simulations, *J. Geophys. Res.*, *113*, A00A10, doi:10.1029/2008JA013239.
- Jordanova, V. K., R. M. Thorne, W. Li, and Y. Miyoshi (2010), Excitation of whistler mode chorus from global ring current simulations, *J. Geophys. Res.*, *115*, A00F10, doi:10.1029/2009JA014810.
- Kennel, C. F., and F. Engelmann (1966), Velocity space diffusion from weak plasma turbulence in a magnetic field, *Phys. Fluids*, *9*(12), 2377–2388.
- Kennel, C. F., and H. E. Petschek (1966), Limit on stably trapped particle fluxes, *J. Geophys. Res.*, *71*(1), 1–28.
- Kim, H. P., J. Hwang, J. J. Seough, and P. H. Yoon (2017), Electron temperature anisotropy regulation by whistler instability, *J. Geophys. Res. Space Physics*, *122*, 4410–4419, doi:10.1002/2016JA023558.
- Nishimura, Y., et al. (2010), Identifying the driver of pulsating aurora, *Science*, *330*(6000), 81–84, doi:10.1126/science.1193130.
- Ossakow, S. L., E. Ott, and I. Haber (1972), Nonlinear evolution of whistler instabilities, *Phys. Fluids*, *15*(12), 2314–2326, doi:10.1063/1.1693875.
- Reeves, G. D., et al. (2013), Electron acceleration in the heart of the Van Allen radiation belts, *Science*, *341*(6149), 991–994, doi:10.1126/science.1237743.
- Seough, J., and P. H. Yoon (2012), Quasilinear theory of anisotropy-beta relations for proton cyclotron and parallel firehose instabilities, *J. Geophys. Res.*, *117*, A08101, doi:10.1029/2012JA017645.
- Shaikh, D., and G. P. Zank (2010), Whistler wave turbulence in solar wind plasma, *AIP Conf. Proc.*, *1216*(1), 180–183, doi:10.1063/1.3395831.
- Smith, E. J., and B. T. Tsurutani (1976), Magnetosheath lion roars, *J. Geophys. Res.*, *81*(13), 2261–2266, doi:10.1029/JA081i013p02261.
- Stansby, D., T. S. Horbury, C. H. K. Chen, and L. Matteini (2016), Experimental determination of whistler wave dispersion relation in the solar wind, *Astrophys. J. Lett.*, *829*(1), 1–5, doi:10.3847/2041-8205/829/1/L16.
- Tao, X. (2014), A numerical study of chorus generation and the related variation of wave intensity using the DAWN code, *J. Geophys. Res. Space Physics*, *119*, 3362–3372, doi:10.1002/2014JA019820.
- Tao, X., and Q. Lu (2014), Formation of electron kappa distributions due to interactions with parallel propagating whistler waves, *Phys. Plasmas*, *21*(2), 022901, doi:10.1063/1.4865574.
- Tao, X., R. M. Thorne, W. Li, B. Ni, N. P. Meredith, and R. B. Horne (2011), Evolution of electron pitch-angle distributions following injection from the plasma sheet, *J. Geophys. Res.*, *116*, A04229, doi:10.1029/2010JA016245.
- Thorne, R. M., E. J. Smith, R. K. Burton, and R. E. Holzer (1973), Plasmaspheric hiss, *J. Geophys. Res.*, *78*(10), 1581–1596.
- Thorne, R. M., B. Ni, X. Tao, R. B. Horne, and N. P. Meredith (2010), Scattering by chorus waves as the dominant cause of diffuse auroral precipitation, *Nature*, *467*, 943–946, doi:10.1038/nature09467.
- Tsurutani, B. T., and E. J. Smith (1974), Postmidnight chorus: A substorm phenomenon, *J. Geophys. Res.*, *79*(1), 118–127.
- Yoon, P. H., and J. Seough (2012), Quasilinear theory of anisotropy-beta relation for combined mirror and proton cyclotron instabilities, *J. Geophys. Res.*, *117*, A08102, doi:10.1029/2012JA017697.
- Yue, C., X. An, J. Bortnik, Q. Ma, W. Li, R. M. Thorne, G. D. Reeves, M. Gkioulidou, D. G. Mitchell, and C. A. Kletzing (2016), The relationship between the macroscopic state of electrons and the properties of chorus waves observed by the Van Allen Probes, *Geophys. Res. Lett.*, *43*, 7804–7812, doi:10.1002/2016GL070084.